Materials Science & Engineering A 585 (2013) 114–122

Contents lists available at ScienceDirect

Materials Science & Engineering A

journal homepage: www.elsevier.com/locate/msea

Evolution of microstructures and mechanical properties during dissimilar electron beam welding of titanium alloy to stainless steel via copper interlayer

I. Tomashchuk [a,*], P. Sallamand [a], N. Belyavina [b], M. Pilloz [a]

[a] Laboratoire Interdisciplinaire Carnot de Bourgogne, UMR 6303 CNRS-Université de Bourgogne, 12 rue de la Fonderie, F-71200 Le Creusot, France
[b] Department of Physics, Taras Shevchenko University, 2, Glushkov Avenue, 03022 Kiev, Ukraine

ARTICLE INFO

Article history:
Received 15 April 2013
Received in revised form
17 July 2013
Accepted 19 July 2013
Available online 31 July 2013

Keywords:
Welding
Titanium alloys
Intermetallics
Electron microscopy
X-ray diffraction
Fracture

ABSTRACT

The influence of operational parameters on the local phase composition and mechanical stability of the electron beam welds between titanium alloy and AISI 316L austenitic stainless steel with a copper foil as an intermediate layer has been studied.

It was shown that two types of weld morphologies could be obtained depending on beam offset from the center line. Beam shift toward the titanium alloy side results in formation of a large amount of the brittle $TiFe_2$ phase, which is located at the steel/melted zone interface and leads to reducing the mechanical resistance of the weld. Beam shift toward the steel side inhibits the melting of titanium alloy and, so, the formation of brittle intermetallics at the titanium alloy/melted zone interface. Mechanical stability of the obtained junctions was shown to depend on the thickness of this intermetallic layer. The fracture zone of the weld was found to be a mixture of TiCu (3–42 wt%), $TiCu_{1-x}Fe_x$ ($x=0.72$–0.84) (22–68 wt%) and $TiCu_{1-x}Fe_x$ ($x=0.09$–0.034) (0–22 wt%). In order to achieve the maximal ultimate tensile strength (350 MPa), the diffusion path length of Ti in the melted zone should be equal to 40–80 μm.

1. Introduction

The high quality dissimilar junctions between titanium alloys and stainless steel have many applications in chemical [1], cryogenic, [2], nuclear [3] and spacecraft [4] industries because of lower cost and weight of the details containing the titanium parts [5].

The main difficulty in joining titanium alloy with steel using fusion is the formation of zones containing the brittle $TiFe_2$ (hardness > 1300 HV [6]) and $TiCr_2$ intermetallics. That is why this approach is not suitable for the direct joining of these materials. The direct joining of this dissimilar couple can be performed only by solid state methods such as diffusion bonding [7–10], friction [3] and explosive [11] welding. The mechanical stability of the weld between titanium and steel can be enhanced by insertion of the intermediate metal foil that changes character of the interaction in the melted zone and leads to formation other phases than Ti–Fe-rich intermetallics.

The development of fusion methods for joining of titanium alloy to steel using an intermediate foil opens an attractive alternative to solid state joining since it allows higher flexibility in geometry of welds, faster welding process and easier preparation of junction surfaces. However, in order to obtain the highest mechanical strength of the joint the following conditions should be satisfied in this case, namely: the material of the inserted foil should be weldable with both alloys; the operational conditions should be optimized in order to maintain the integrity of this interlayer before the solidification; the local composition should be optimized to prevent the formation of large zones with brittle phases.

The conventional fusion welding methods such as arc welding are not suitable for this purpose because of the formation of long lifetime melted zones with strong mixing of the components. The instability of electric arc makes it difficult to maintain a continuous energy supply that in turn leads to local variations of the melted zone content. The high power beam methods such as laser and electron beam welding are more suitable for joining dissimilar alloys because they provide very local heat supply, rapid heating/cooling gradients and a perfect precision in the weld realization. Both methods were successfully applied for welding of different dissimilar couples in [12–14].

It is known that titanium does not form intermetallic phases with pure Zr, Nb, Mo, Ta, V and Hf, which could be tested as potential interlayers. Good result was also obtained in [15] with pure Ag as interlayer despite the formation of the AgTi intermetallic which is not brittle [16]. The high cost of all these metals

* Corresponding author. Tel.: +33 3 85 73 11 23, +33 6 18 29 52 85; fax:+33 3 85 73 11 20.
E-mail addresses: iryna.tomashchuk@u-bourgogne.fr, iryna84@hotmail.fr (I. Tomashchuk).

0921-5093/$ - see front matter © 2013 Elsevier B.V. All rights reserved.
http://dx.doi.org/10.1016/j.msea.2013.07.050

and problems of their weldability with stainless steel result in use of more available materials such as Cu [5], Ni [17] and their alloys. However, in this case the risk of embrittlement of the weld due to intermetallic phase formation is high enough and titanium/foil interface appears to be the weakest part of the joint. Good results were obtained for infrared bonding of titanium to stainless steel with combined V/Cr/Ni interlayer (here Cr/Ni foil contacts with the stainless steel to prevent the brittle σ-phase of the V–Fe system and V foil contacts with titanium) [18]. The first attempts to use vanadium and tantalum interlayers for CO_2 laser welding have not being successful because of the oxidation problems and formation of the brittle phases [19].

Despite the formation of numerous intermetallic phases in the Cu–Ti system [20], copper is often used as interlayer material for joining titanium alloys to steels due to the compensation of local phase brittleness by ductility of copper. As the Cu–Fe system [21] does not contain intermetallic phases, it is easy to create mechanically stable copper–steel junctions both by solid state (diffusion bonding [22]) and fusion (electron beam [23] and laser [24]) methods. The formation of a narrow reaction zone between titanium and copper, in which the Cu–Ti intermetallics are formed, allows successful joining by explosion welding [25] and diffusion bonding [5,26]. In case of joining by fusion, thin copper foil cannot be able to prevent Ti–Fe interaction completely and therefore the whole Fe–Cu–Ti interaction takes place resulting in five ternary phases [27]. Because of numerous phases formed in the melted zone the optimization of phase composition of the joint becomes a difficult task.

The first attempt to perform fusion welding of titanium alloy to steel with copper interlayer (1 mm thickness) was made by Wang et al. [28]. The junction was obtained by two-pass electron beam welding and melted zone was shown to contain $TiFe_2$ intermetallics dispersed in the copper medium. The mechanical resistance of the weld was equal to 224 MPa and the brittle fracture within intermetallic layer occurred near the titanium/melted zone interface. Previous study [29] of the welding of Ti6Al4V to austenitic stainless steel by both pulsed Nd:YAG laser and electron beam have shown the possibility of one-pass joining with a use of 0.5 mm thick copper foil. In both cases, the shift of heat source to copper–steel interface has allowed reduce the melting of the titanium alloy. The total metallurgical isolation of welded materials by copper interlayer was not achieved. However, the existence of the miscibility gap in the Cu–Fe system [30,31] and rapid cooling of the melt [23,31] resulted in formation of the immiscible flows and droplets between liquid copper and steel that enhanced the barrier function of the foil. The mechanical resistances of the electron beam and pulsed Nd:YAG laser welds were found to be similar (UTS about 350 MPa). This conformity was determined by similar structures of the inner intermetallic layers between Ti6Al4V and melted zone. Close result was obtained by Wang et al. [32] for welding of AISI 304L with Ti6Al2Mo2V2Zr alloy. By use of CO_2 laser Pugacheva et al. [33] have carried out welding of titanium and stainless steel via copper interlayer with injected of TiN and Y_2O_3 nanoparticles, which allowed to disperse brittle intermetallics and attain the UTS of 375 MPa. However, only a few welding conditions were tested in these studies.

In this paper, the influence of operational parameters of electron beam welding of titanium alloy to austenitic stainless steel with use of 0.57 mm thick copper interlayer is explored. The influence of heat source shift and of welding speed on weld morphology, phase content and mechanical resistance of the joint was studied in order to define the optimal structure of dissimilar interfaces.

2. Experimental procedure

2.1. Materials

2 mm thick austenitic stainless steel AISI 316L, 2 mm thick α–β titanium alloy and 572 ± 4 μm thick copper foil were used as raw materials. Their chemical and phase compositions are listed in Table 1.

2.2. Welding method

Electron beam welding was carried out in a key-hole mode using Techmeta S.A. welding machine with maximal beam power of 6 kW and spot diameter of 400 μm. The acceleration voltage of welding was 25 kV and beam current was 40 mA. The electron beam was focused at the surface of butt joint.

The welding configuration is given in Fig.1. The beam offset varied relatively to zero point in the center of the interlayer from 0.25 mm towards titanium alloy to 0.7 mm towards AISI 316L steel (offset to the titanium alloy side was considered as negative and to AISI 316L side – as positive). The constant offset values were used for each prepared weld (Table 2).

2.3. Characterization methods

The cross sections of the welds were polished and attacked by the Kalling's reagent. 20 mm large transversal cuts of the weld

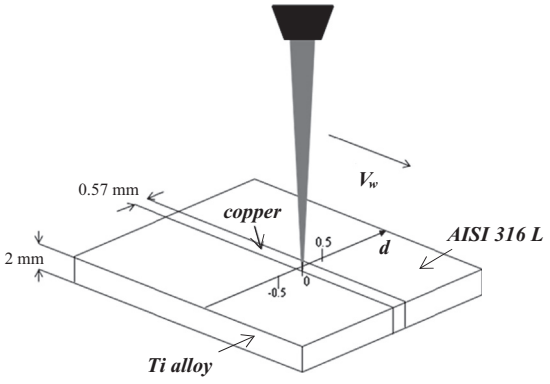

Fig.1. The configuration of welding with different beam offset (*d*).

Table 1
Chemical and phase composition of welded materials.

Material	Chemical composition (at%)									Phase composition and lattice constants (nm)		
	Al	Ti	V	Cr	Fe	Ni	Cu	Mn	Si	Phases	*a*	*c*
AISI 316L	–	–	–	20	68	7	0	balance		γ-Fe (100 wt%)	0.35937	–
Oxygen-free copper	–	–	–	–	–	–	100	–	–	Cu (100 wt%)	0.36146	–
Ti alloy	9	87	4	–	–	–	–	–	–	α-Ti (95 wt%)	0.29237	0.46685
										β-Ti (5 wt%)	0.32104	–

were undergone tensile test. The fractured surfaces from both sides of broken welds were examined.

The microstructure and chemical composition of the samples were studied by scanning electron microscope (JEOL) with fast EDS analyzer.

The identification of phase composition on the fractured surfaces and on the polished cuts was carried out by the X-ray diffraction (PANalytical X'Pert PRO) using a cobalt target. The scanning range of 40–95° with a step scan of 0.0167° and counting time of 200 s per step were used. The shaping of the X-ray beam by the application of appropriate slits allowed to scan whole fracture surface (20×2 mm^2). The peak positions and integral intensities of the observed reflections were determined by the full profile analysis. The original software package with special banks for the X-ray diffraction data of intermetallic and inorganic compounds was used [34] to carry out the qualitative and semi-quantitative (wt%) phase analysis in order to determine the phase compositions and to define the lattice constants of the identified phases and solid solutions.

Table 2
Welding parameters and averaged chemical composition of the melted zones.

Beam offset from interlayer center (mm)	Welding speed (m/min)	Averaged chemical composition (at%)					
		Ti	Fe	Cr	Ni	Cu	Al, V, Mn, Si
−0.25	1.8	19	2	1	1	76	Balance
0	1.8	20	13	3	1	62	
0.25	1.8	10	50	6	2	29	
0.5	1.8	7	31	6	2	53	
0.7	1.8	No fusion at the Ti alloy side					
0.25	1.0	22	26	8	1	41	
0.25	2.5	1	43	9	4	43	
0.25	3.0	Lack of fusion at the Ti alloy side					

The UTS of the welds was evaluated at room temperature in tensile testing machine (MTS Insight 30 kN) at a cross head speed of 8.3×10^{-5} m/s. Four tests by weld were made.

3. Results and discussion

3.1. General observation

In the case of dissimilar welding with an interlayer foil [35], the beam offset (d) (Fig.1) is a key-parameter to control the proportion between melted materials, while the welding speed (V_w) influences mostly on the length of the melted zone (MZ) and, thus, it defines the lifetime of the melt [35]. To vary the composition of the melted zone five different values of beam offset from joint center line and three values of linear speed were applied. Obtained data for melted zone chemical compositions are listed in Table 2.

The welding tests show that for a fixed welding speed (1.8 m/min) the materials can be assembled within an offset range between −0.25 mm (lack of fusion at AISI 316L side) and 0.7 mm (no fusion at titanium alloy side). Defect-free melted zones (about 1 mm width) can be obtained within this range. According to EDS data, they contain mainly Cu, while the amounts of Ti and Fe strongly depend on the welding parameters (very small amount of Cr and Ni are found in the melted zone). The transversal X-ray elemental maps of the welds are given at Fig. 2.

The study of the melted zone contents reveals that the change of beam offset (from negative to positive) under constant welding speed (1.8 m/min) leads to stepwise decrease of the content of titanium alloy elements and rapid increase of the content of steel elements. Earlier the same step-wise variations of global MZ contents were mentioned in the study of the copper–steel electron beam welding [36]. In [36] this phenomenon was explained both by the difference between the physical properties of the welded materials and the position and shape of the cylindrical vaporization zone.

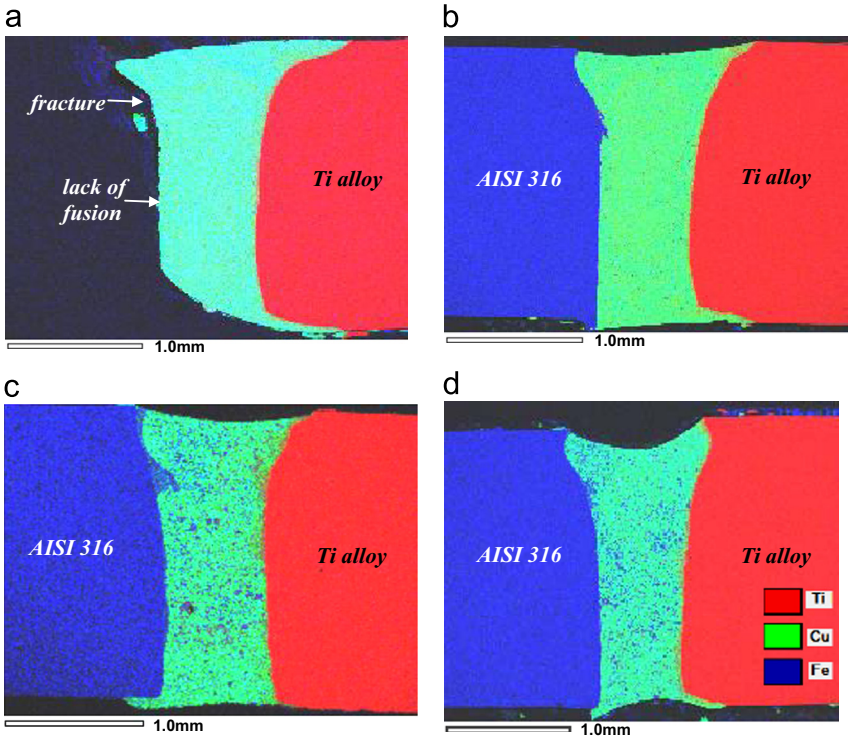

Fig. 2. X-ray distribution element maps in the welds performed with a different beam offsets: −0.25 mm (a), 0 mm (b), 0.25 mm(c) and 0.5 mm (d) (welding speed of 1.8 m/min).

Two characteristic MZ morphologies can be observed. It is seen that the welds performed with $d \leq 0$ (Fig. 2a and b) are enriched in uniformly distributed titanium alloy elements (≈ 20 at% Ti and ≤ 13 at% Fe). On the contrary, the welds performed with $d > 0$ (Fig. 2c and d) are enriched in steel elements (> 30 at% Fe and ≤ 10 at% Ti), which form numerous inclusions in the copper medium.

The influence of welding speed on the melted zone content is studied under fixed beam offset (0.25 mm). Low welding speed provides almost equal fusion of both steel and titanium alloy sides and a homogenous distribution of the components in the copper medium (Fig. 3a). Increase of the welding speed leads to decrease of the titanium alloy melting as well as to increase of the steel element amounts (Fig. 3b). Our numerical study [35] showed that in case of positive beam offset the steel side of the weld was eroded by copper-rich flow. Since the velocity of this flow is proportional to the V_w, the increase of welding speed leads to more intense erosion and melting of the steel side. It could be confirmed by the presence of large zones of liquid steel torn away from the steel/MZ interface (Fig. 3b). For slower V_w, this flow only starts to form (Fig. 2 c).

3.2. Microstructure observation

Three characteristic zones of the weld cross sections are studied: the middle of the melted zone, the Ti/MZ interface and the steel/MZ interface.

3.2.1. Influence of beam offset

The step-wise change of global MZ composition with beam offset results in two different sets of phases that can be found in MZ of steel-rich (Fig. 4a) and Ti-rich welds (Fig.4b).

For steel-rich welds (Fig. 2c and d), melted steel is distributed in copper medium in form of globular inclusions (Fig. 4a), caused by the miscibility gap in Cu–Fe system. These globular inclusions are in fact the solid solutions on the base of γ-Fe and contain up to 8 at% Cu which lead to increase of their lattice constants from $a=0.35937$ nm for stainless steel (Table 1) to $a=0.36425$ nm for solid solution (Table 3 and Fig. 5a). Obtained value of Cu solubility in steel inclusions corresponds to the solubility of Cu in γ-Fe at 1084 °C (fusion temperature of copper) [37]. So, during welding copper medium interacts with molten steel forming solid solution which becomes supersaturated under higher cooling rate. The solubility of Fe in the Cu-rich medium of MZ is low and according to EDS analysis is about 4 at% Fe. It is found that some titanium (15 at% Ti) is located in the Fe-rich zones as $TiFe_2$ inclusions and only 1 at% Ti is localized in Cu-rich medium. This fact could be explained by higher chemical affinity of Ti with Fe than with Cu. It is found that Cr does not migrate from γ-Fe-rich globules to Cu-rich medium because of its low solubility in Cu. Only small amount of nickel is located in the copper medium of the weld in spite of good solubility in Cu. So, the minor steel elements such as Ni and Cr do not migrate into the Cu interlayer because of short lifetime of the melted zone typical for electron beam welding.

For Ti-rich welds (Fig. 2a and b), the melted zone is formed by two main phases (Fig.4b) confirmed by XRD (Fig.5b), namely, the Cu-rich solid solution (up to 8 at% Ti) and Cu_3Ti_2 intermetallic. The solidus temperature of such Cu-rich solid solution (close to 1085 °C [38]) is higher than the melting temperatures of Cu–Ti intermetallics (890 °C for Cu_3Ti_2 [38]), therefore it solidifies primarily in the form of large dendrites. The Cu_3Ti_2 intermetallic is located among these dendrites in a form of small inclusions and contains up to 7–8 at% Fe, according to EDS analysis. So, one can suppose the formation of the ternary phase τ_2 ($Ti_{40}Fe_xCu_{60-x}$, $x=5$–17), which is isostructural with Cu_3Ti_2. Fig.4b displays that the space between τ_2 inclusions and Cu-rich dendrites is filled with the eutectic-like disperse mixture.

Due to variety of chemical composition of across the weld, numerous intermetallics of titanium form at the Ti/MZ interface under different welding conditions. Their combination has a strong

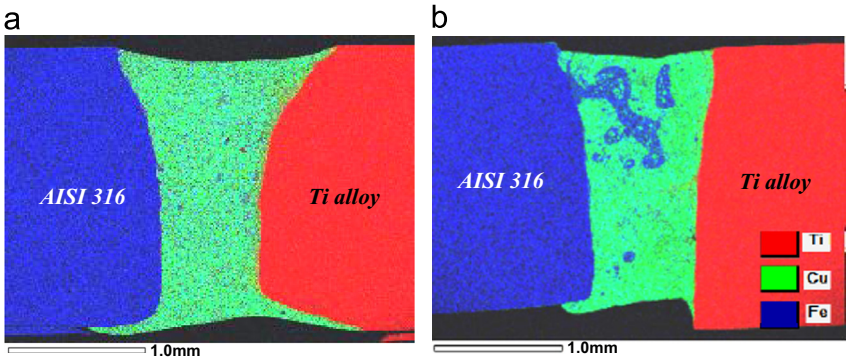

Fig. 3. X-ray distribution element maps in the welds performed with a different welding speeds: 1 m/min (a) and 2.5 m/min (b) (beam offset of 0.25 mm).

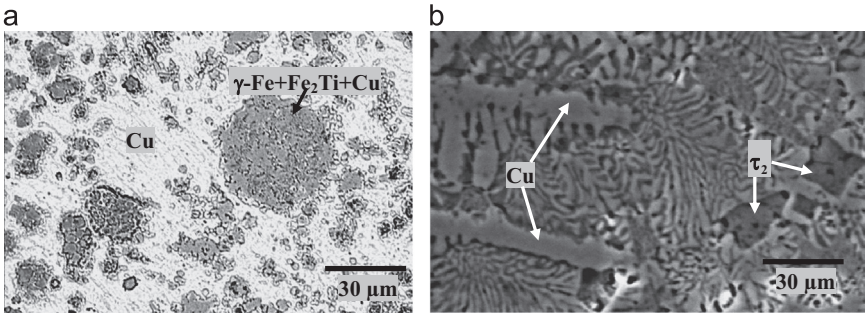

Fig. 4. The microstructures of the MZ of the welds performed with a different beam offsets: 0.25 mm (a) and −0.25 mm (b) (welding speed of 1.8 m/min).

Table 3
The phase composition[a] of the fracture zones according to XRD and EDS analysis.

Beam offset (mm)	V_w (m/min)	Fracture location					
		Ti alloy side		MZ side		AISI 316L side	
		XRD[b]	EDS[c]	XRD[b]	EDS[c]	XRD[b]	EDS[c]
−0.25	1.8			γ-$Fe_{1-x}Cu_x$ – 47% Cu – 38% $TiFe_2$ – 15%	Fe_2Ti Cu	γ-Fe	Fe
0	1.8			γ-$Fe_{1-x}Cu_x$ – 93% $TiFe_2$ – 7%	Fe_2Ti γ-Fe Cu	γ-Fe – 90% $TiFe_2$ – 8% γ-$Fe_{1-x}Cu_x$ – 2%	Fe Fe_2Ti
0.25	1.8	TiFe – 39% TiFe′ – 22% α-Ti – 16% γ-$Fe_{1-x}Cu_x$ –1 2% TiCu – 3%	FeTi CuTi$_2$	TiFe – 51% TiFe′ – 31% γ-$Fe_{1-x}Cu_x$ – 9% TiCu – 9%	FeTi CuTi$_2$ CuTi		
0.5	1.8	TiCu –3 4% α-Ti –2 4% γ-$Fe_{1-x}Cu_x$ –1 9% TiFe – 23%	FeTi CuTi$_2$ CuTi	TiCu – 15% γ-$Fe_{1-x}Cu_x$ – 68% TiFe – 17%	FeTi CuTi$_2$ CuTi		
0.25	1.0	TiFe – 68% TiCu – 13% α-Ti – 18% $TiFe_2$ – 2% TiFe′ – 2%	FeTi CuTi$_2$ Ti	TiFe – 55% γ-$Fe_{1-x}Cu_x$ – 18% TiCu – 18% Cu – 4% $TiFe_2$ – 5%	FeTi CuTi$_2$ CuTi		
0.25	2.5	Ti alloy	Ti	TiCu – 42% TiFe – 37% TiFe′ – 15% $TiFe_2$ – 4% Cu – 2%	FeTi CuTi$_2$ CuTi		

[a] γ-Fe in fact is the γ-Fe_xCu_{1-x} solid solution with a=0.363–0.364 nm; TiFe and TiFe′ in fact are the $TiFe_xCu_{x-1}$ solid solutions with a=0.307–0.308 nm and a=0.3020–0.3030 nm, respectively.
[b] Phase content is given in wt%.
[c] The phases predicted from local EDS measurements and Ti–Cu–Fe phase diagram.

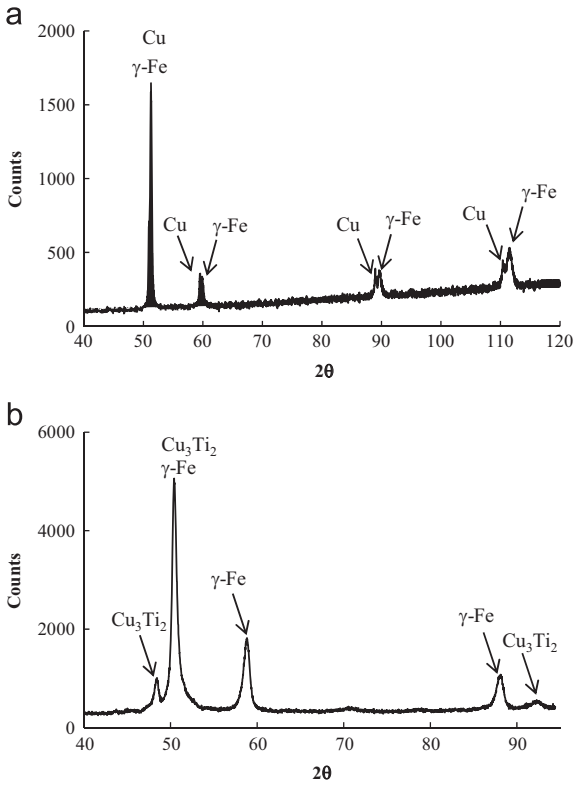

Fig. 5. The X-ray patterns of the MZ of the welds performed with a different beam offsets: 0.25 mm (a) and −0.25 mm (b) (welding speed of 1.8 m/min).

influence on the strength of the weld. It was shown (Fig. 6a–c) that the formation of a thin layer of the Ti-rich intermetallics takes place for any beam offset. In turn, the competing diffusion flows of steel elements and Cu penetrate into the Ti-rich melted region forming the multiple layers with different phase compositions. Taking into account the temperatures of the phase formations (Cu, γ-Fe and intermetallics) one can conclude that the Ti/MZ interface solidifies the last. So, crystallization of the γ-Fe and Cu solid solutions puts obstacles for steel element fluxes from the MZ side and therefore solidification of the liquid in the trap starts from titanium alloy side.

The inner interface layers in the titanium alloy side are similar. The formation of the existing phases could be explained by the following local invariant reactions:

$$L+\alpha\text{-}Ti \Rightarrow TiFe+Ti_2Cu\ (990\ ^\circ C)$$

$$L+Ti_2Cu \Rightarrow TiFe+CuTi\ (950\ ^\circ C)$$

On the contrary, the outer layers have different phase compositions depending on Ti and Fe content in the melted zone.

It is found that low amounts of minor steel elements (Cr, Ni) are present in the Ti/MZ interface. No Cr- and Ni-containing intermetallics are detected.

According to EDS and XRD, the AISI 316L/MZ interface contains γ-Fe solid solution (8 at% Cu) and a small amount of $TiFe_2$ (Fig. 6d–f), which rises with increase of titanium content in the MZ (the interface with beam offset of $d=-0.25$ mm contains up to 20 at% Ti and with one of d=0.25 mm contains only 3 at% Ti).

3.2.2. Influence of welding speed

For a fixed beam offset of 0.25 mm, the decrease in the welding speed from 2.5 m/min to 1 m/min leads to increase of titanium amount in the MZ. However, the high content of Fe (Table 2), comparing to case of $d \leq 0$, prevents the bulk formation of Cu–Ti intermetallics in the middle of MZ (Fig.7a). In case of low speed (1 m/min) Ti is concentrated (20–35 at% Ti) in the steel-rich inclusions and forms the mixture of three Cu-containing solid solutions (on the basis of γ-Fe, TiFe and $TiFe_2$ phases) while the copper medium contains only 4 at% Ti. High welding speed

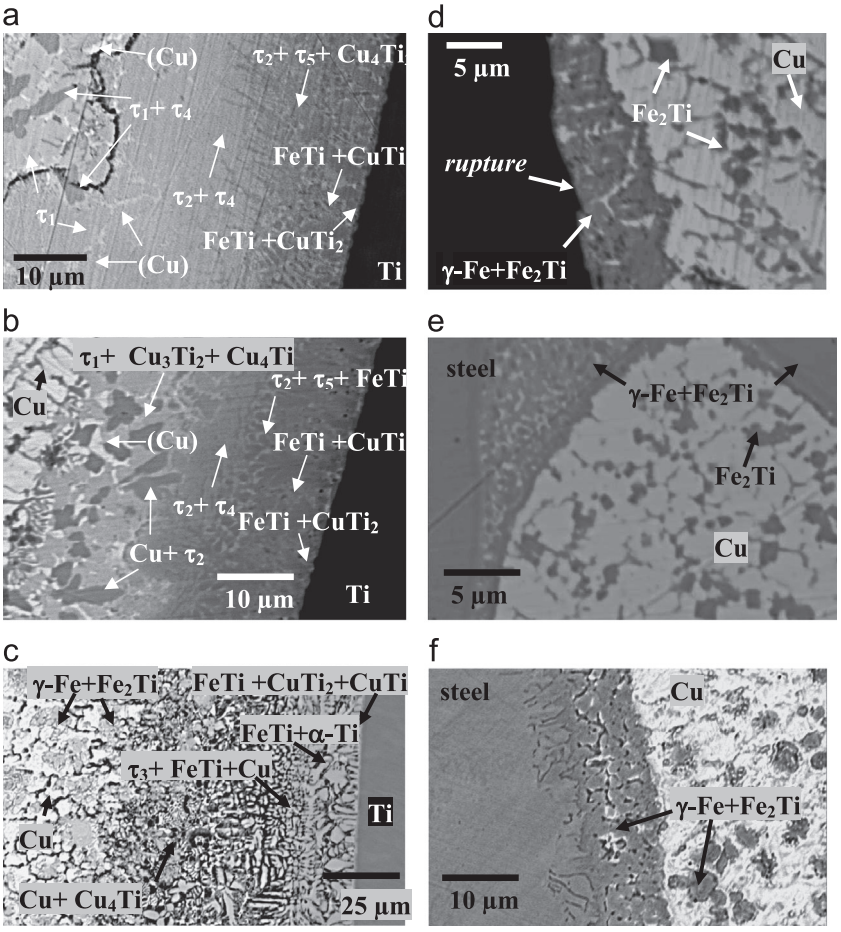

Fig. 6. The microstructures both of the Ti/MZ (a–c) and steel/MZ (d–f) interfaces of the welds performed with a different beam offsets: −0.25 mm (a and d), 0 mm (b and e) and 0.25 mm (c and f) (welding speed of 1.8 m/min).

(2.5 m/min) leads to extreme decrease of Ti content in MZ. Consequently, only two phases (Cu and γ-Fe) are present in the center of MZ (Fig.7d).

The solubility of Cu in the steel-rich globules increases proportionally to Ti content. For example, at low welding speed (1 m/min) the steel globules with 35 at% Ti dissolve up to 18 at% Cu while those ones with 20 at% Ti dissolve only 13 at% Cu (according to EDS analysis). At the higher welding speeds the solubility of Cu in the steel-rich inclusions decrease to 8 at%. It could be supposed that at low welding speed (1 m/min) increase of Cu solubility is attributed to the formation of TiFe that can dissolve up to 38 at% Cu [39].

Decrease of the welding speed corresponds to increase of the lifetime of the melt and, so, it influences the thickness of the intermetallic at Ti/MZ interface, namely, 16, 66 and 93 μm thicknesses for welding speed of 2.5, 1.8 and 1 m/min, respectively. For all welding speeds the inner interface layers from titanium alloy side have the similar phase composition (Ti_2Cu+CuTi+FeTi) while phase compositions of the outer layers are different from each others. The outer layers under V_w=2.5 m/min (Fig. 7e) contain only Cu–Ti intermetallics which corresponds to their interdiffusion profile of Cu and Ti. For V_w=1 m/min (Fig.7b) the outer layers are enriched in Fe–Ti intermetallics.

The AISI 316L/MZ interface contains the solid solution of Cu in γ-Fe (about 8 at% Cu, Fig. 7c and f) regardless of the welding speed. It is found that these interfaces contain 24, 3 and 2 at% Ti for the welding speeds of 1, 1.8 and 2.5 m/min, respectively. In the first case, the formation of $TiFe_2$ takes place (Table 3).

3.3. Mechanical properties

The tensile test (Table 4) reveals two fracture modes. It is found that the welds performed with negative beam offset ($d \leq 0$) are fractured at AISI 316L/MZ interface, while all joints with positive beam offset ($d > 0$) are fractured at Ti/MZ interface. The values of strain remain low for all welding conditions, which corresponds to a brittle fracture. The highest values of UTS and strain (340–350 MPa and 4.25–4.5%, respectively) were obtained for a beam offset d=0.25–0.5 mm and the for welding speed 1.8 m/min. Any changes in the welding speed lead to decrease of the UTS values (Table 4).

The fracture surfaces were studied by SEM–EDS and XRD analysis in order to estimate the correlation between local microstructures (phase compositions) and mechanical properties.

Brittle fracture can be observed (Fig. 8) at AISI 316L/MZ interface. According to XRD the main phases on the fracture edge at MZ side are the solid solutions of γ-Fe and Cu (Table 3). The presence of $TiFe_2$ affects the stability of this interface. One can see that under beam offset of −0.25 mm the cracking of AISI 316L/MZ interface occurs during solidification in presence of 15 wt% $TiFe_2$ while under zero beam offset the defect-free AISI 316L/MZ interface that contains 7 wt% $TiFe_2$ is stable. The AISI 316L side of the fracture is enriched in a pure austenite. This fact reveals that fracture occurs very close to solid steel.

Brittle fracture is observed at Ti/MZ interface of the weld prepared under beam offset of d=0.25 mm and welding speed of 1.8 m/min (Fig. 9a). Under lower welding speed (1.0 m/min) the

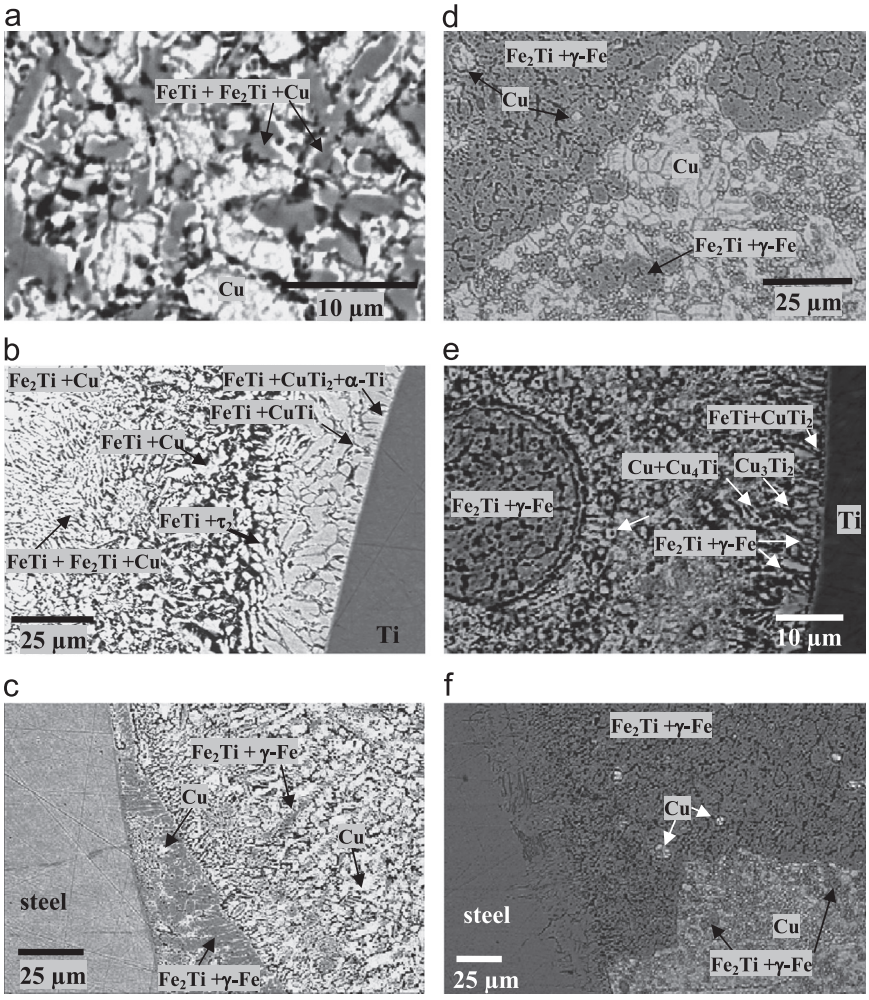

Fig. 7. The microstructures of MZ (a and d), at the Ti/MZ interface (b and e) and at the steel/MZ interface (c and f) of the welds performed with a different welding speed: 1 m/min (a–c) and 2.5 m/min (d–f) (beam offset of 0.25 mm).

Table 4
The results of tensile test.

Beam offset from interlayer center (mm)	Welding speed (m/min)	Fracture position	UTS (MPa)
Variations of the beam offset			
−0.25	1.8	Steel/MZ interface	0
0	1.8	Steel/MZ interface	195 ± 5
0.25	1.8	Ti/MZ interface	350 ± 6
0.5	1.8	Ti/MZ interface	340 ± 5
0.7	1.8	No welding at AISI 316L side	0
Variations of the welding speed			
0.25	1	Ti/MZ interface	163 ± 7
0.25	1.8	Ti/MZ interface	350 ± 6
0.25	2.5	Ti/MZ interface	258 ± 7
0.25	3	No welding at Ti side	0

morphology of the fractured surface changes that could be explained by a higher thickness of Ti-rich layer under this welding condition. The floral-like cleavage facets can be observed (Fig. 9b).

The Ti/MZ fractures contain the mixture of TiFe, TiCu, γ-Fe, $TiFe_2$ and some amount of Ti_2Cu (Table 3) from both the titanium alloy and the MZ sides, except the weld prepared under d=0.25 mm and V_w=2.5 m/min, where the titanium alloy side contain α-Ti only.

The main phases formed at Ti/MZ fracture surfaces are TiCu and TiFe. It is shown that TiFe intermetallic dissolves some amount of Cu forming ternary solid solutions with increased lattice constants (Table 3). Taking into account the linear dependence of the lattice constants of this solid solution via Cu content [40], it is possible to estimate Cu content in $TiCu_{1-x}Fe_x$ for each case. The γ-Fe solid solution is also often detected. The increase of their lattice constants (0.3622–0.3650 nm) is found to be correlated with the EDS analysis (8 at% Cu in γ-Fe solid solution). The identification of little amounts of Ti–Cu intermetallics in their mixture is difficult, so the Ti_2Cu compound, which should be form in this zone due to invariant reactions [27], is not detected.

TiFe solid solution is the main phase at the fracture surfaces of the weld performed with a beam offset of 0.25 mm (Table 3). In fact, there are two $TiCu_{1-x}Fe_x$ solid solutions with different Cu contents which are estimated by the lattice constant values: namely, $TiCu_{0.27}Fe_{0.73}$ (3/5 part) and $TiCu_{0.62}Fe_{0.34}$ (2/5 part). Low amount (< 10 wt%) of TiCu and some amount of γ-Fe solid solution were also found at this interface.

The fracture edge of the weld performed under beam offset of 0.5 mm contains smaller amount of Fe, while the amount of TiCu content is higher (up to 34 wt%) and only one TiFe-based solid solution is formed (23 wt% Cu, $TiCu_{0.2}Fe_{0.8}$). However, these features do not affect the UTS value essentially.

The decrease of welding speed down to 1 m/min and enrichment of MZ by both titanium alloy and AISI 316L elements lead to domination of the $TiCu_{1-x}Fe_x$ phases (70 wt%). Two of these solid

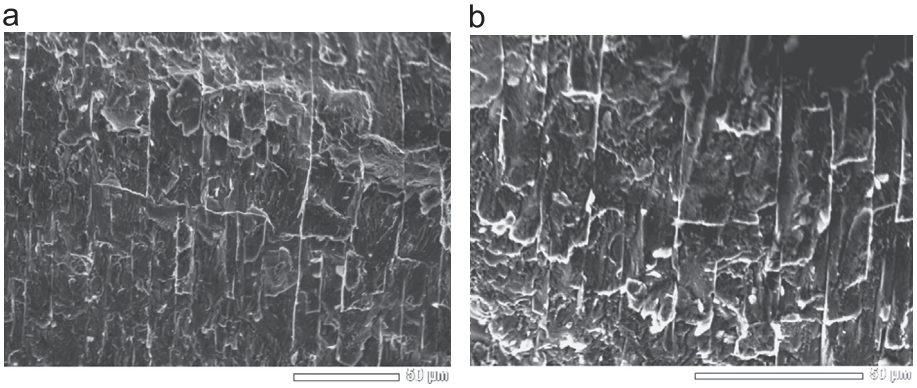

Fig. 8. The fractography of the weld broken at AISI 316/MZ interfaces: welding speed 1.8 m/min and beam offset of −0.25 mm (a) and of 0 mm (b).

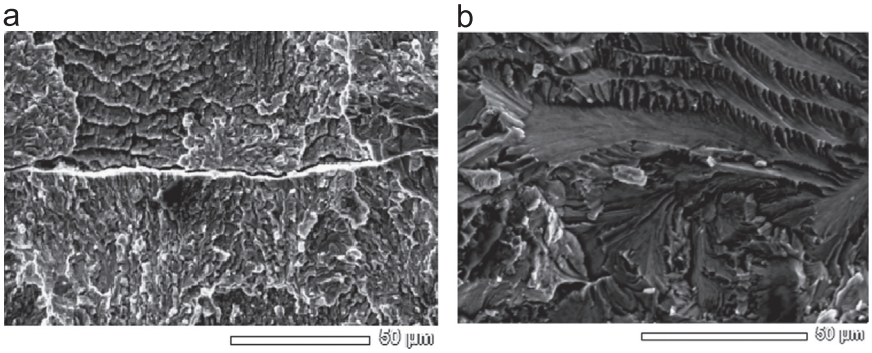

Fig. 9. The fractography of the welds broken at Ti/MZ interface performed with beam offset of 0.25 mm and different welding speeds: 1.8 m/min (a) and 1 m/min (b) (MZ side).

solutions can be found on the fracture edges, namely, $TiCu_{0.28}Fe_{0.72}$ and $TiCu_{0.51}Fe_{0.49}$. The amount of TiCu in MZ increases to 13–18 wt %. Some α-Ti, $TiFe_2$ and γ-Fe solid solution are detected at the titanium alloy and MZ fracture sides.

The increase of welding speed up to 2.5 m/min leads to the clean fracture between titanium alloy and MZ: only α-Ti solid solution was found at the titanium alloy side. The TiCu intermetallic dominates at the fracture edge (42 wt%) because of low amount of Fe in the MZ. There are two TiFe solid solutions (37 wt% of $TiCu_{0.16}Fe_{0.84}$ and 15 wt% of $TiCu_{0.91}Fe_{0.09}$) as well as some amount of Cu and $TiFe_2$.

It is found that the variation of the proportions between Cu and Fe-containing intermetallics present in the fracture zone does not affect the mechanical properties if their amounts are following: 3–42 wt% for TiCu, 22–68 wt% for $TiCu_{1-x}Fe_x$ (x=0.72–0.84) and 0–22 wt% for $TiCu_{1-x}Fe_x$ (x=0.09–0.034). However, the thickness of intermetallic layer at Ti/MZ interface (estimated basing on SEM images (Figs. 6a–c and 7b and e) and EDS) affects the values of UTS (Fig. 10). These data are supplemented by our previous result obtained in close welding conditions [29]. UTS values decrease when the thickness of intermetallic layers is outside the range of 40–80 μm. One could explain that as follows. On the one hand, if the intermetallic layer is too thin, the interface suffers from the lack of interaction and it is not stable, so the titanium alloy detaches itself. On the other hand, if the interface is too large, the mechanical stability of the weld suffers from the accumulation of layered brittle intermetallic which is mechanically inhomogeneous.

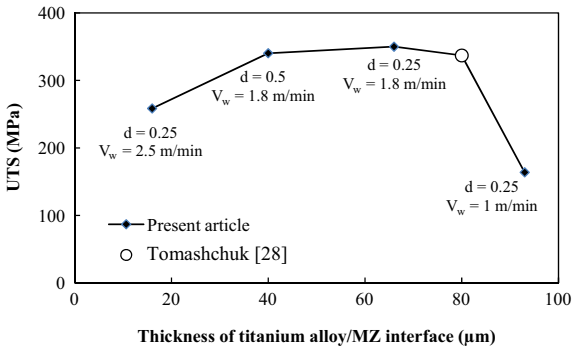

Fig. 10. The variation of UTS in function of the thickness of Ti/MZ interface.

4. Conclusions

The parametric study of electron beam joining of titanium alloy to stainless steel AISI 316L via 570 μm copper interlayer has been carried out. The influence of beam offset and welding speed on the composition, microstructure and mechanical resistance of the joints has been studied. Important conclusions are summarized below.

1. The welds prepared either with zero beam offset or with offset on titanium alloy side contains mostly the Cu-rich dendrites and τ_2 ternary phase. The fracture occurred at the steel/MZ interface embrittled by the accumulation of brittle $TiFe_2$. The UTS value obtained for this type of fracture (d=0 mm, V_w=1.8 m/min) was equal to 195 MPa, which corresponds to formation of 7% $TiFe_2$. The interface between titanium alloy and melted zone contained compact layers of Cu–Fe–Ti intermetallics and was more stable than the interface between melted zone and steel.
2. The beam offset at the steel side resulted in melted zones containing γ-Fe globular inclusions and Cu-rich medium. A small amount of dispersed $TiFe_2$ was found in these welds. The diffusion of Ti into melted zone was limited to compact

layer formed by intermetallic phases. In this case, no considerable accumulation of $TiFe_2$ took place at the interface between melted zone and steel. The fracture occurred at the interface between titanium alloy and melted zone. The fracture edges were found to be composed by the mixture of TiCu [3–42 wt%] and $TiCu_{1-x}Fe_x$ with $x=0.72$–0.84 [22–68 wt%] and $x=0.09$–0.034 [0–22 wt%]. The UTS of 350 MPa can be obtained by beam offset of 0.25–0.5 mm on steel side.

3. The analysis of the experimental results showed that mechanical stability of the joints performed with beam offset to steel side depends on the diffusion path length in the Ti-rich interface. The optimal value of diffusion path length was found to be 40–80 μm, which can be obtained, for the Cu interlayer of 570 μm, under high welding speed (≈ 2 m/min) and the positioning of the electron beam at the interface between copper interlayer and steel.

References

[1] C. Church, R.K. Wied, J. Vac. Sci. Technol. A 16 (1998) 1885–1889.
[2] B. Shanmugarajan, G. Padmanabham, Opt. Lasers Eng. 50 (2012) 1621–1627.
[3] H.C. Dey, M. Ashfaq, A.K. Bhaduri, K.Rao Prasad, J. Mater. Process. Technol. 209 (2009) 5862–5870.
[4] R.R. Boyer, Mat. Sci. Eng. A 213 (1996) 103–114.
[5] A. Elrefaey, W. Tillmann, J. Mater. Process. Technol. 209 (2009) 2746–2752.
[6] O.G. Bykovskiy, I.V. Tkachenko, Paton Weld. J. 9 (1987) 414.
[7] S. Kundu, S. Sam, S. Chatterjee, Mater. Sci. Eng. A 528 (2011) 4910–4916.
[8] M. Ghosh, S. Chatterjee, B. Mishra, Mater. Sci. Eng. A 363 (2003) 268–274.
[9] M. Ghosh, S. Das, P.S. Banarjee, S. Chatterjee, Mater. Sci. Eng. A 390 (2005) 217–226.
[10] S. Kundu, M. Ghosh, S. Chatterjee, Mater. Sci. Eng. A 428 (2006) 18–23.
[11] N. Kahraman, B. Gülenç, F. Findik, J. Mater. Process. Technol. 169 (2005) 127–133.
[12] A. Mathieu, R. Shabadi, A. Deschamps, M. Suery, S. Matteï, D. Grevey, E. Cicala, Opt. Lasers Technol. 39 (2007) 652–661.
[13] S. Chatterjee, T.A. Abinandanan, K. Chattopadhyay, Mater. Sci. Eng. A 490 (2008) 7–15.
[14] Z. Sun, R. Karppi, J. Mater. Process. Technol. 59 (1996) 257–267.
[15] E. Atasoy, N. Kahraman, Mater. Charact. 59 (2008) 1481–1490.
[16] M.K. Lee, J.G. Lee, J.K. Lee, J.J. Park, G.J. Lee, Y.R. Uhm, C.K. Rhee, J. Mater. Res. 23 (2008) 2254–2263.
[17] S. Kundu, S. Chatterjee, Mater. Sci. Eng. A 425 (2006) 107–113.
[18] M.K. Lee, J.G. Lee, Y.H. Choi, D.W. Kim, C.K. Rhee, Y.B. Lee, S.J. Hong, Mater. Lett. 64 (2010) 1105–1108.
[19] B. Shanmugarajan, G. Padmanabham, Opt. Lasers Eng. 50 (2012) 1621–1627.
[20] H. Okamoto, J. Phase Equilib. 26 (2002) 549–550.
[21] W. Oelsen, E. Schurmann, C. Florin, Arch. Eisenhuttenwes 32 (1961) 719–728.
[22] O. Yilmaz, M. Askoy, J. Mater. Process. Technol. 121 (2002) 136–142.
[23] I. Magnabosco, P. Ferro, F. Bonollo, L. Arnberg, Mater. Sci. Eng. A 424 (2006) 163–173.
[24] T.A. Mai, A.C. Spowage, Mater. Sci. Eng. A 374 (2004) 224–233.
[25] W.-B. Lee, Y.-J. Kim, S.-B. Jung, Intermet 12 (2004) 671–678.
[26] S. Kundu, M. Ghosh, A. Laik, K. Bhanumurthy, G.B. Kale, S. Chatterjee, Mater. Sci. Eng. A 407 (2005) 154–160.
[27] T. Velikanova, M. Turchanin, Ternary Alloy Systems. Phase Diagrams, Crystallographic and Thermodynamic Data, in: G. Effenberg, S. Ilyenko (Eds.), Springer, Berlin, 2008, pp. 15–31.
[28] T. Wang, B. Zhang, G. Chen, J. Feng, Q. Tang, Trans. Nonferr. Met. Soc. China 20 (2010) 1829–1834.
[29] I. Tomashchuk, P. Sallamand, H. Andrzejewski, D. Grevey, Intermet 19 (2011) 1466–1473.
[30] G. Wilde, J.H. Peperezko, Acta Mater. 47 (1999) 3009–3021.
[31] Y.Z. Chen, F. Liu, G.C. Yang, X.Q. Xu, Y.H. Zhou, J. Alloys Compd. L1–L5 (2007) 427.
[32] T. Wang, B. Zhang, J. Feng, Q. Tang, Mater. Charact. 73 (2012) 104–113.
[33] N.B. Pugacheva, S.V. Smirnov, D.I. Vichuganin, Yu V. Afonin, A.M. Orishich, S.M. Zadvorkin, L.S. Goruleva, Deform. Razrush. Mater. 7 (2012) 26–32.
[34] V. Markiv, N. Belyavina, in: Proceedings of the Second International Scientific Conference of Engineering and Functional Materials, 14–16 October 1997, L'viv, Ukraine, p. 260.
[35] I. Tomashchuk, P. Sallamand, J.M. Jouvard, J. Mater. Process. Technol. 211 (2011) 1796–1803.
[36] I. Tomashchuk, P. Sallamand, J.M. Jouvard, D. Grevey, Comput. Mater. Sci. 48 (2010) 827–836.
[37] N.P. Lyakishev, Phase Diagrams of Binary Metallic Systems, Mashinostroenie, Moscow, 2001.
[38] H. Okamoto, J. Phase Equilib. 26 (2002) 549–550.
[39] V. Raghavan, J. Phase Equilib. 23 (2002) 172–174.
[40] C. Wu, J. Li, Metall. Trans. A 20A (1989) 981–985.